Communications
doi.org/10.1002/batt.202000117

Chemistry Europe
European Chemical Societies Publishing

VIP *Very Important Paper*

A High-Rate and Long-Life Rechargeable Battery Operated at −75 °C

Xiaoli Dong,*[a] Yang Yang,[a] Panlong Li,[a] Zhong Fang,[a] Yonggang Wang,[a] and Yongyao Xia*[a, b]

Intercalation compounds are commonly-used electrodes for commercialized lithium ion batteries (LIBs), while suffering from the sluggish interfacial processes at subzero temperature. Herein, nanoscale Nb_2O_5 has been investigated as a viable cathode for rechargeable batteries operated at the temperature of as low as −75 °C. Benefitting from the surface-controlled charge storage process, the intrinsic intercalation pseudocapacitance of Nb_2O_5 broke the rate limitation at low temperature. Particularly, the battery exhibited outstanding rate performance (100 C) at room temperature and delivered high a reversible charge/discharge with a high capacity of 121 mAh g^{-1} at −75 °C. Furthermore, a capacity retention of 50% and a long life for 100 cycles without capacity fading were achieved with a rate of 0.5 C at such low temperature. Based on the outstanding electrochemical performance from −75 °C to +25 °C, it can be envisaged that materials with intercalation pseudocapacitive behavior could be served as good candidate for energy storage systems under extreme conditions.

As one of the most important members of electrochemical energy storage systems, lithium-ion batteries (LIBs) have been widely used in modern life. However, the drastically performance fading at subzero temperature limited their application in extreme conditions including high-altitude areas, cold terrains, polar/military/space exploration, and so on.[1–5] Various factors have been considered to affect the low temperature electrochemical performance, including decreased ionic conductivity of the electrolyte, sluggish solid state diffusion in the bulk electrodes, difficult Li-ions de-solvation process and increased charge transfer resistance at the electrolyte/electrode interphase.[6–9] Among them, the decreased ionic conductivity of electrolyte is generally described as the primary limitation. During the past decades, great efforts have been paid to modify electrolyte for low temperature application, such as liquefied gas electrolyte, fluorinated electrolytes and co-solvent electrolytes,[2,3,10–12] which lead to significant improvement of discharge performance. Unfortunately, the discharge process is often limited to small rate and the charge process is rarely reported at low temperature. Charging a discharged LIB is more difficult than discharging of a charged LIB, attributed to the slow interfacial processes.[13–16] The sluggish de-solvation and charge transfer greatly impeded the operation of conventional intercalation compounds at sub-zero fields,[17–21] not to mention the high rate and long cycle investigations. Therefore, it is urgently desired to develop advanced materials for rechargeable batteries at low temperature.

Generally, energy-storage materials can be classified for batteries and capacitors according to their fundamentally different electrochemical reaction mechanisms. The former behaved high energy through diffusion-limited faradaic redox reactions with slow charging (hours-level), while the latter exhibited high power through the surface-controlled ion adsorption of electrical double layers that is very fast (seconds-level). In between them, intercalation pseudocapacitive materials combine the battery-like redox reactions and fast kinetics not limited by semi-infinite diffusion, which called surface-controlled faradaic reactions.[22,23] Therefore, they involve the diffusion of ions within the bulk material, while it is faster and no phase change compared with conventional intercalation compounds.[23,24] The unique surface-controlled intercalation behavior might be beneficial to circumvent the challenge of sluggish Li^+ de-solvation and diffusion processes from the electrolyte to the bulk electrode, offering as a candidate substitution of conventional intercalation compounds at low temperature.[25] Researchers discovered the Li^+ intercalation pseudocapacitive mechanism in orthorhombic phase Nb_2O_5,[26–28] which delivers fast insertion kinetics through a pseudocapacitive reaction of Li^+ on the surface of the electrode in nonaqueous electrolytes accompanied by an intercalation reaction.[29,30] In view of such characterizations, Nb_2O_5 material could be highly suitable for charge storage at low temperature, which has never been investigated up to now.

Herein, we proposed the important application of Nb_2O_5 to demonstrate a rechargeable battery with excellent low temperature performance. The kinetics of charge storage at ultra-low temperature (−75 °C) was firstly quantified through cyclic voltammetry (CV), which turned out to be a surface-controlled process. A high capacity of 95 mAh g^{-1} can be reached even with fast charge in 36 seconds (corresponding to a high rate of

[a] Dr. X. Dong, Y. Yang, P. Li, Z. Fang, Prof. Y. Wang, Prof. Y. Xia
Department of Chemistry and Shanghai Key Laboratory of Molecular Catalysis and Innovative Materials,
Institute of New Energy,
iChEM (Collaborative Innovation Center of Chemistry for Energy Materials)
Fudan University
Shanghai 200433, China
E-mail: xldong@fudan.edu.cn
yyxia@fudan.edu
[b] Prof. Y. Xia
College of Chemistry and Molecular Engineering,
Zhengzhou University,
Zhengzhou 450001, China

Supporting information for this article is available on the WWW under https://doi.org/10.1002/batt.202000117

100 C) at +25 °C. Even when the temperature was reduced to −75 °C, the battery can deliver a high capacity of 121 mAh g^{-1} and long life for 100 cycles without obvious capacity fading. In addition, the power density can reach 1178 W kg^{-1} at −75 °C, offered a possibility for developing high power batteries within a wide temperature range from −75 °C to +25 °C.

The Nb_2O_5 powder was prepared through an aqueous sol-gel method according to previous literature.[26] X-ray diffraction (XRD) pattern was collected to investigate the crystallographic structure of the material. As shown in Figure 1a, all XRD peaks can be assigned and well consistent with the orthorhombic structure of T-Nb_2O_5 (JCPDS No. 30-0873).[27] The unique (001) reflection can be used to determine the lattice parameter along the *c*-axis, which was estimated to be 3.90 Å, close to the theoretical value of 3.93 Å.[27] A feature has been demonstrated that the (001) planes offer energetically favorable pathways for the facile transport of Li^+ in the structure.[31] The differential scanning calorimetry (DSC) measurement was carried out to reveal its thermal endurance, especially at low temperature (Figure 1b). No endothermal or exothermal behavior was observed from −120 °C to +20 °C, indicating its structural stability within a wide temperature range. The average particle size was about 35 nm as presented in Figure 1c, corresponding to that from TEM (Figure S1). The nanoscale is a great benefit to preserve the atomic-scale behavior for electrochemical performance. The magnification of the TEM image clearly detected the crystal lattice (Figure 1d and Figure S2), which was measured approximately as 4.06 Å, conforming to that obtained with XRD. The surface area was about 17 m^2 g^{-1} (Figure S3). The well prepared nanosized structure and thermal stability of such Nb_2O_5 are the prerequisites for its electrochemical performance at low temperature.

An ethyl acetate (EA)-based co-solvent electrolyte was applied to detect the charge storage behavior of Nb_2O_5 electrode, owing to its stability and wide operation temperature range.[12] Voltammetry response investigations were carried out with a three-electrode system in which Nb_2O_5 micro-electrode (Figure S4) acted as work electrode and two Li foils were used as counter and reference electrodes, respectively. The charge-storage process is based on the intercalation of Li^+ into Nb_2O_5 accompanied with the reduction of Nb^{5+} to Nb^{4+} [Eq. (1)]:

$$Nb_2O_5 + xLi^+ + xe^- \rightleftharpoons Li_xNb_2O_5 \quad (1)$$

in which the maximum value of x is 2, corresponding to a maximum theoretical capacity of about 201.7 mAh g^{-1}. The insertion of Li^+ into Nb_2O_5 occurs at below 2 V (vs. Li^+/Li), which can be demonstrated with the cyclic voltammetry (CV) characterizations (Figure S5). The CV curves at different scan rates from 0.05 mV s^{-1} to 35 mV s^{-1} were presented in Figure 2a. The peak current (i_p, mA) and scan rate (v, mV s^{-1}) generally obey the following power-law relationship: $i_p = av^b$ in which both a and b are adjustable parameters. A b-value of 0.5 usually indicated a semi-infinite linear diffusion-controlled process (battery behavior), and the *b*-value of 1 corresponded to a surface-controlled reaction (capacitive behavior). It can be detected from the relationship of response current with sweep rate (Figure 2b) that the *b*-value is 0.92 and 0.93 for the insertion and extraction processes, respectively. This indicated the fast Li^+ intercalation while the current is linearly proportional to the scan rate, implying the surface-controlled kinetics of the intercalation behavior. The charge contribution from the capacitive-controlled (k_1v) and diffusion-controlled ($k_2v^{1/2}$) can be divided and quantified according to Equations (2) and (3):

$$i = k_1v + k_2v^{1/2} \quad (2)$$

$$i/v^{1/2} = k_1v^{1/2} + k_2 \quad (3)$$

The values of k_1 and k_2 at each potential can be determined by the line fitting of the $i/v^{1/2}$ *vs* $v^{1/2}$ plot. The capacitive contribution (k_1v) can be therefore calculated out based on the

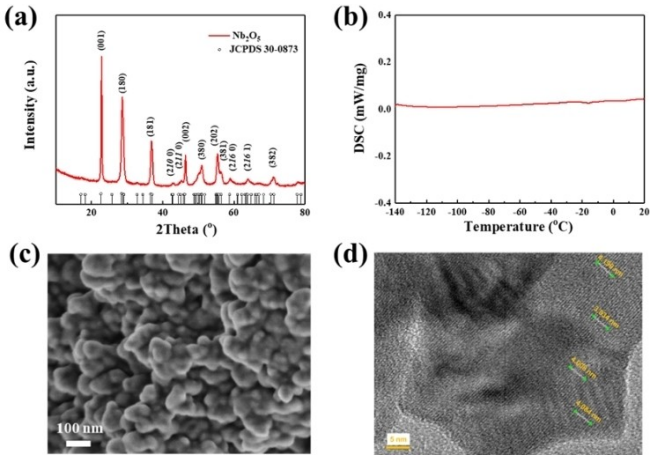

Figure 1. Characterizations of the as-prepared Nb_2O_5 powder. a) XRD pattern; b) DSC with the temperature range from −120 °C to +20 °C; c) SEM image; d) TEM image.

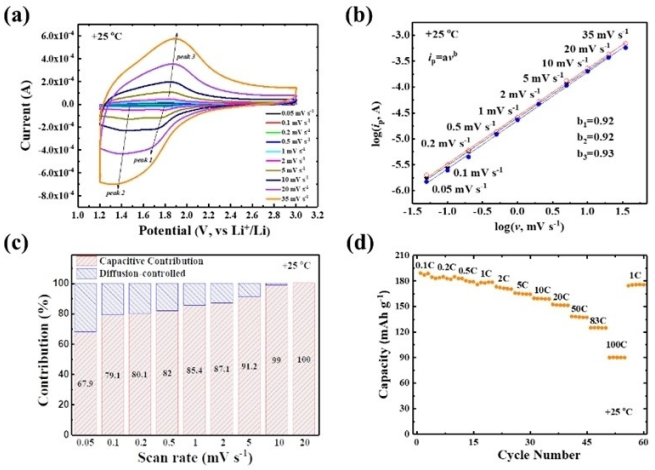

Figure 2. Electrochemical performance of Nb_2O_5 at ambient temperature of +25 °C. a) Kinetics investigation with CV curves at various scan rates; b) the log relationship of peak current *vs.* scan rate; c) capacitive contribution; d) rate performance of the Nb_2O_5-based battery.

integral area ratio at each specific potential. As displayed in Figure 2c, it can be detected that the major capacity was contributed from the dominant capacitive process, where the surface-controlled capacitive contribution was about 85.4% at the scan rate of 1 mV s^{-1} (Figure S6a).It should be mentioned that the contribution from surface adsorption should be small owing to its low surface area. When increasing the scan rate to 20 mV s^{-1}, the capacitive contribution ratio reached near 100% (Figure S6b), which well demonstrated the capacitive behavior. The quantitative analysis of the b values and capacitive contribution clearly disclosed the typical intercalation pseudocapacitive process of Nb_2O_5, during which the faradaic contribution occurs at very short timescales while the diffusion-related processes are expected to be minimal.[28] The charge/discharge performance with different current densities was shown in Figure 2d and Figure S7. A high capacity of 188 mAh g^{-1} can be obtained with the 0.1 C, close to its theoretical capacity. The capacity was well remained at a higher rate of 1 C (178 mAh g^{-1}), and only a slight decrease at 5 C (166 mAh g^{-1}). When charged in 43 seconds (corresponding to 83 C-rate), the battery can still deliver a high capacity of 125 mAh g^{-1}. Even charged with 100 C, the capacity still reached 95 mAh g^{-1}, indicating a superior rate performance. Such a high rate capability can be attributed to its intercalation pseudocapacitive behavior. Besides, the Nb_2O_5 cathode also behaved excellent cycle performance, with a high capacity retention of 92% after 200 cycles with 1 C charge/discharge at room temperature (Figure S8).

Inspired by the outstanding high rate performance, we are wondering whether the pseudocapacitive behavior can benefit the low temperature operation. Therefore, the kinetics and electrochemical processes are conducted at low temperature. It should be mentioned that Nb_2O_5 film electrode was used for the Swagelok T-cell three-electrode system operated at low temperature, owing to the failure of the fragile micro-electrode at the super low temperature. It is astonishing to find that the pseudocapacitive behavior can be well preserved even at an ultra-low temperature of −75 °C, as depicted from Figure S9. The difference existed in that only one pair of redox peaks can be observed, caused by the increased polarization with the temperature decline. This trend can be further diagnosed through the electrochemical impedance spectroscopy (EIS) investigations at +25 °C and −75 °C (Figure 3a and **3 b**). The EIS curves mainly consist of the ohmic resistance (R_s) in high frequency, two depressed semicircles in the high-to-middle frequency representing the interfacial resistance (R_{SEI}) and charge transfer resistance (R_{ct}), a slop line at low frequency corresponding to the solid-state diffusion.[32] Accordingly, two sets of resisters and capacitors connected in parallel were used for the equivalent circuit (Figure 3c). To make a direct comparison, the resistances at different temperatures were figured out in Figure 3d. All the resistance showed a negative correlation with the temperature, which increased at low temperatures. It can be detected that the resistance from charge transfer became much larger than that at +25 °C, which controlled the overall polarization at low temperature. The activation energy, E_a, represents the barrier that Li^+ needs to

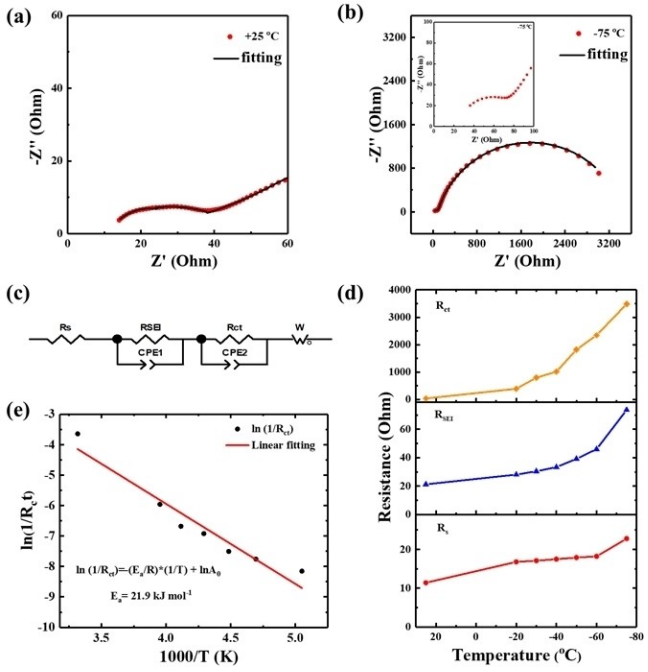

Figure 3. EIS investigations at various temperatures. Experimental curve and simulation curve at +25 °C (a) and −75 °C (b); c) the equivalent circuit; d) the comparison of R_s, R_{SEI}, and R_{ct} with the temperature decreasing; e) the plot of ln ($1/R_{ct}$) vs. (1000/T) to obtain E_a value.

overcome for the Li^+ charge transfer process. The value of E_a can be determined from the relationship: $1/R_{ct} = A_0 e^{-Ea/RT}$, in which A_0, R and T are a frequency factor, the gas constant and the temperature in Kelvin, respectively. The plot of ln ($1/R_{ct}$) vs. (1000/T) in Figure 3e indicated that the E_a was 21.9 kJ mol^{-1} (approximately 0.23 eV). The value of R_{ct} and is much lower than that of commonly used intercalation compounds, such as LMO and LTO (Figure S10). For better comparison, the E_a for LMO and LTO were calculated as 43 kJ mol^{-1} and 37 kJ mol^{-1}, respectively, which is consistent with previous reports .[33–36] In addition, the symmetric cells of Nb_2O_5 with 50% state of charge were applied to eliminate the contribution of the shared Li-metal anode to the charge transfer impedance (Figure S11). The resistance from Nb_2O_5 cathode turned out to be small at the temperature of −75 °C, which might be attributed to the low energy barriers from (001) plane for ion transports and activation barriers compared to other lithium-ion battery materials.[37,38] The voltammetry studies and EIS results can well demonstrate the feasibility of Nb_2O_5 at low temperature.

In the next logic step, we further examined the electrochemical performance, including its specific capacity, rate capability and cycle performance at low temperature. The capacity was calculated out based on the mass of Nb_2O_5 cathode. As shown in Figure 4a, the charge/discharge curves at −75 °C can be observed with different current densities. The battery showed a high capacity of 121 mAh g^{-1} at the 0.05 C rate, approximately 64% of the capacity at +25 °C. The capacity retention kept about 50% with a higher rate of 0.5 C at −75 °C. Excellent rate performance from 0.05 C to 5 C displayed its fast kinetics benefitting from its pseudocapacitive insertion behav-

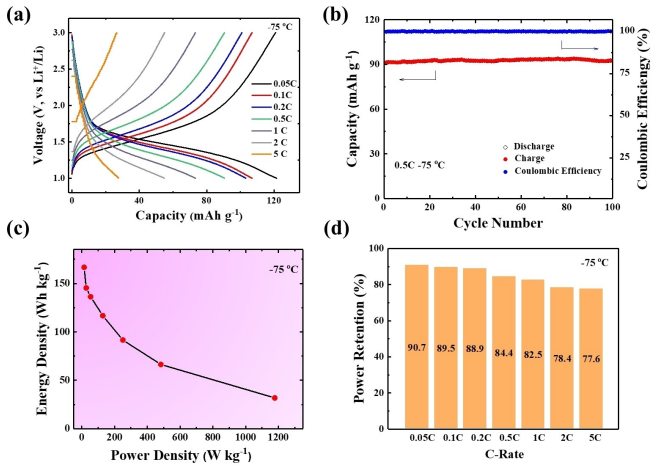

Figure 4. Electrochemical performance of Nb_2O_5 at low temperature. a) charge/discharge curves with various rates at −75 °C; b) cycle performance with 0.5 C; c) Ragone plot and d) retention of the power density at −75 °C compared to that obtained at +25 °C.

ior, which is much higher than the reported at low temperature (< −40 °C, Table S1). Cycle stability was explored with the current density of 0.5 C (Figure 4b), almost no capacity fading can be detected over 100 cycles. This might be driven by the surface-controlled charge storage process, which offered a possible solution to circumvent the difficulty facing intercalation compounds at low temperature. Moreover, it's worth mentioning that the cycle performance at low temperature has never been investigated, because traditional LIBs based on intercalation compounds can barely be recharged at −40 °C. Energy density and power density were accordingly estimated based on the total mass of Nb_2O_5 cathode and consumed Li anode, as depicted in the Ragone plot (Figure 4c). A high power density can be obtained with 1178 W kg^{-1} at the rate of 5 C. To make a direct observation of the power capability at low temperature, the retention was figured out as Figure 4d in comparison with that at +25 °C (Figure S12 and detailed calculation). The high power retention of 90.7% can be achieved at 0.05 C and still keep as high as 77.6% at 5 C, indicating the favorable power ability at low temperature. It can be concluded that the intercalation pseudocapacitive behavior of Nb_2O_5 showed outstanding low-temperature endurance and realized the superior electrochemical performance within a wide temperature range from −75 °C to +25 °C. The application of Nb_2O_5 offered a possibility to construct high power rechargeable battery at low temperature.

In summary, we presented a high power rechargeable battery with outstanding low temperature performance by applying Nb_2O_5 as cathode. The intercalation pseudocapacitive behavior was demonstrated to maintain even at the low temperature, which contributed greatly to the excellent performance of the rechargeable battery. The surface-controlled process drove the fast transport of Li^+, enabling the battery with high capacity of 121 mAh g^{-1} and high power density of 1178 W kg^{-1} at −75 °C. Moreover, the battery exhibited superior cycle stability with the coulombic efficiency of ~100% during the 100 cycles at such low temperature. Based on the comprehensive consideration of electrochemical performance from −75 °C to +25 °C, materials with pseudocapacitive insertion could be served as a candidate for energy storage systems under extreme conditions. Moreover, benefitting from the unique charge-storage behavior, the sluggish desolvation process that impeded the operation of intercalation compounds at low temperature might be resolved if tuning the coating structure of Nb_2O_5 on the out-surface in the future.

Acknowledgements

This work was supported by the National Natural Science Foundation of China (21875045, 21935003), National Key Research and Development Plan (2016YFB0901500), Chenguang Program supported by Shanghai Education Development Foundation and Shanghai Municipal Education Commission (19CG01).

Conflict of Interest

The authors declare no conflict of interest.

Keywords: ultra-low temperature of −75 °C · rechargeable battery · high rate · long life · intercalation pseudocapacitive behavior

[1] C. Y. Wang, G. S. Zhang, S. H. Ge, T. Xu, Y. Ji, X. G. Yang, Y. J. Leng, *Nature* **2016**, *529*, 515–518.
[2] C. S. Rustomji, Y. Yang, T. K. Kim, J. Mac, Y. J. Kim, E. Caldwell, H. Chyng, Y. S. Meng, *Science* **2017**, *356*, aal4263.
[3] X. L. Fan, X. Ji, L. Chen, J Chen, T. Deng, F. D. Han, J. Yue, N. Piao, R. X. Wang, X. Q. Zhou, X. Z. Xiao, L. X. Chen, C. S. Wang, *Nat. Energy* **2019**, *4*, 882–890.
[4] X. L. Dong, Z. W. Guo, Z. Y. Guo, Y. G. Wang, Y. Qi, Y. Y. Xia, *Joule* **2018**, *2*, 902–913.
[5] S. S. Zhang, K. Xu, T. R. Jow, *Electrochem. Commun.* **2002**, *4*, 928–932.
[6] M. T. F. Rodrigues, G. Babu, H. Gullapalli, K. Kalaga, F. N. Sayed, K. Kato, J. Joyner, P. M. Ajayan, *Nat. Energy.* **2017**, *2*, 17108.
[7] J. Xu, X. Wang, N. Y. Yuan, J. N. Ding, S. Qin, J. M. Razal, X. H. Wang, S. H. Ge, Y. Gogotsi, *Energy Storage Mater.* **2019**, *23*, 383–389.
[8] G. L. Zhu, K. C. Wen, W. Q. Lv, X. Z. Zhou, Y. C. Liang, F. Yang, Z. L. Chen, M. D. Zou, J. C. Li, Y. Q. Zhang, W. D. He, *J. Power Sources* **2015**, *300*, 29–40.
[9] J. B. Hou, M. Yang, D. Y. Wang, J. L. Zhang, *Adv. Energy Mater.* **2020**, 1904152.
[10] M. C. Smart, J. F. Whitacre, B. V. Ratnakumar, K. Amine, *J. Power Sources* **2007**, *168*, 501–508.
[11] M. C. Smart, B. V. Ratnakumar, K. B. Chin, L. D. Whitcanack, *J. Electrochem. Soc.* **2010**, *157*, A1361–A1374.
[12] X. L. Dong, Y. X. Lin, P. L. Li, Y. Y. Ma, J. H. Huang, D. Bin, Y. G. Wang, Y. Qi, Y. Y. Xia, *Angew. Chem. Int. Ed.* **2019**, *131*, 5679–5683.
[13] J. Holoubek, Y. J. Yin, M. Q. Li, M. Y. Yu, Y. S. Meng, P. Liu, Z. Chen, *Angew. Chem. Int. Ed.* **2019**, *58*,18892–18897.
[14] S. S. Zhang, K. Xu, T. R. Jow, *J. Power Sources* **2003**, *115*, 137–140.
[15] S. S. Zhang, K. Xu, T. R. Jow, *Electrochim. Acta* **2004**, *49*, 1057–1061.
[16] G. J. Xu, S. Q. Huang, Z. L. Cui, X. F. Du, X. Wang, D. Lu, X. H. Shangguan, J. Ma, P. X. Han, X. H. Zhou, G. L. Cui, *J. Power Sources* **2019**, *416*, 29–36.
[17] T. R. Jow, S. A. Delp, J. L. Allen, J. P. Jones, M. C. Smart, *J. Electrochem. Soc.* **2018**, *165*, A361–A367.
[18] K. Xu, Y. F. Lam, S. S. Zhang, T. R. Jow, T. B. Curtis, *J. Phys. Chem. C.* **2007**, *111*, 7411–7421.

[19] T. Abe, H. Fukuda, Y. Iriyama, Z. Ogumi, *J. Electrochem. Soc.* **2004**, *151*, A1120-A1123.
[20] B. K. Zou, H. Y. Wang, Z. Y. Qiang, Y. Shao, X. Sun, Z. Y. Wen, C. H. Chen, *Electrochim. Acta* **2016**, *196*, 377–385.
[21] X. L. Wu, Y. G. Guo, J. Su, J. W. Xiong, Y. L. Zhang, L. J. Wan, *Adv. Energy Mater.* **2013**, *3*, 1155–1160.
[22] C. Choi, D. S. Ashby, Q. L. Wei, J. Lau, B. Dunn, *Nat. Rev. Mater.* **2020**, *5*, 5–19.
[23] V. Augustyn, P. Simon, B. Dunn, *Energy Environ. Sci.* **2014**, *7*, 1597.
[24] Y. Q. Jiang, J. P. Liu, *Energy Environ. Mater.* **2019**, *2*, 30–37.
[25] X. L. Dong, Y. Y. B. L. Wang, Y. J. Cao, N. Wang, P. L. Li, Y. G. Wang, Y. Y. Xia, *Adv. Sci.* **2020**, 2000196.
[26] V. Augustyn, J. Come, M. A. Lowe, J. W. Kim, P. L. Taberna, S. H. Tolbert, H. D. Abruña, P. Simon, B. Dunn, *Nat. Mater.* **2013**, *12*, 518–522.
[27] K. Brezesinski, J. Wang, J. Haetge, C. Reitz, S. O. Steinmueller, S. H. Tolbert, B. M. Smarsly, B. Dunn, T. Brezesinski, *J. Am. Chem. Soc.* **2010**, *132*, 6982–6990.
[28] J. W. Kim, V. Augustyn, B. Dunn, *Adv. Energy Mater.* **2012**, *2*, 141–148.
[29] H. W. Wang, C. R. Zhu, D. L. Chao, Q. Y. Yan, H. J. Fan, *Adv. Mater.* **2017**, *29*, 1702093.
[30] B. H. Deng, T. Y. Lei, W. H. Zhu, L. Xiao, J. P. Liu, *Adv. Funct. Mater.* **2018**, *28*, 1704330.
[31] R. Kodama, Y. Terada, I. Nakai, S. Komaba, N. Kumagai, *J. Electrochem. Soc.* **2006**, *153*, A583–A588.
[32] T. Osaka, D. Mukoyama, H. Nara, *J. Electrochem. Soc.* **2015**, *162*, A2529-A2537.
[33] T. Huang, D. Mukoyama, H. Nara, N. Takami, T. Momma, T. Osaka, *J. Power Sources* **2013**, *222*, 442–447.
[34] P. Suresh, A. K. Shukla, N. Munichandraiah, *J. Appl. Electrochem.* **2002**, *32*, 267–273.
[35] D. M. Wu, *Ionics* **2012**, *18*, 559–564.
[36] H. Ishikawa, O. Mendoza, Y. Sone, M. Umeda, *J. Power Sources* **2012**, *198*, 236–242.
[37] J. Come, V. Augustyn, J. W. Kim, P. Rozier, P. L. Taberna, P. Gogotsi, J. W. Long, B. Dunn, P. Simon, *J. Electrochem. Soc.* **2014**, *161*, A718–A725.
[38] K. J. Griffith, A. C. Forse, J. M. Griffin, C. P. Grey, *J. Am. Chem. Soc.* **2016**, *138*, 8888–8899.

Manuscript received: May 25, 2020
Revised manuscript received: June 8, 2020
Accepted manuscript online: June 9, 2020
Version of record online: July 7, 2020